

# The distortion of a magnetic field by flow in a shock tube

By M. D. COWLEY

Department of Engineering, University of Cambridge

(Received 23 June 1961)

Induced magnetic fields in shock-tube flows have been measured by previous authors, in order to determine the electrical conductivity of ionized gases. Distortion of the applied magnetic field was taken to be small. In the present work, the full magnetic field solution is developed for idealized boundary conditions. At a magnetic Reynolds number equal to 4 the distortion is found to be considerable, but the field is well represented by a solution correct to third order in magnetic Reynolds number. The axial field in a real shock-tube configuration was computed, and experimentally measured fields were found to agree reasonably with theory.

---

## 1. Introduction

The electrical conductivity of an ionized gas can be found experimentally from the currents induced in the gas when it flows through a magnetic field. This technique was used by Lin, Resler & Kantrowitz (1955) to determine the conductivity of argon. The flow of ionized argon was generated in a shock-tube, and the magnetic field was applied by means of a d.c. coil, mounted so that its axis coincided with that of the shock-tube. Recently Pain & Smy (1960) have made similar measurements of the conductivity of argon using a shock tube and two pulsed field coils. In both these experiments, the magnitude of currents in the gas was deduced from the pick-up on a search coil, and the response was calibrated by comparison with the response due to materials of known conductivity. The analyses of the results concentrated on the fact that the sample of gas has a finite length over which the conductivity is not constant. This variation occurs since there is a small region behind the shock in which the gas has not reached equilibrium, and there is a subsequent cooling of the gas with 'bremstrahlung' radiation.

In principle the induced currents can be calculated from the interaction of the flow with only the applied field if the conductivity and velocity distributions are known, and the currents are not strong enough to modify the applied field appreciably. The induced field at the search coil can be determined by Biot-Savart's law. It is well known that such a technique is valid when the magnetic Reynolds number is small, i.e.

$$R_M = \mu\sigma vl \ll 1, \quad (1)$$

where  $\mu$  is the permeability,  $\sigma$  the electrical conductivity,  $v$  the velocity,  $l$  a typical length, and the M.K.S. system is being used. However, except in small,

low-speed shock-tubes the condition (1) is not valid, and it is the purpose of the present paper to investigate the distortion of magnetic fields as the condition is relaxed. If we can express the field solution as a power series in  $R_M$ ,

$$\mathbf{B} = \mathbf{B}_0 + R_M \mathbf{B}_1 + R_M^2 \mathbf{B}_2 \dots, \quad (2)$$

where  $\mathbf{B}_0$  is the applied field, interest lies in the second- and higher-order terms. Although the analysis of Lin *et al.* (1955) assumed the condition (1), their search coil was calibrated over a range of values of  $R_M$ . In their case the second- and higher-order effects were found to be negligible, and could be discounted.

We shall assume here that the applied magnetic field is weak so that the electrical conductivity is scalar, and magnetic forces have negligible effect on the flow pattern. The latter condition requires that

$$C_M = \frac{\sigma B^2 l}{\rho v} \ll 1, \quad (3)$$

where  $B$  is a typical field strength, and  $\rho$  is the gas density. The problem is then idealized by assuming that there is steady uniform flow down the tube, the electrical conductivity is constant, and the gas sample has infinite length. This idealization is reasonable if the applied field region is short compared to the length over which the conductivity changes appreciably, and the rise of the induced field is rapid. The magnetic field is taken to be axially symmetric with only radial and longitudinal components, as might be given by coils or systems of coils whose axes coincide with the shock-tube axis.

Kinematic problems in magnetohydrodynamics, for which the velocity field and conductivity distribution are assumed to be known, have been treated by many authors, notably Lundquist (1952). Usually there have been no boundaries to the velocity field, and in a previous paper, Cowley (1961), the simple solution for a wire loop or coil was given. Here the problem is more difficult. The kinematic solution within the shock-tube must be compatible with a free-space solution outside. However, as a first step towards understanding the higher-order effects in  $R_M$  we may assume that the magnetic flux at the wall of the tube can be measured, and the problem reduces to that of finding a kinematic solution for a known boundary condition. In practice the magnetic flux at a high-conductivity metal wall will be held constant for the duration of flow in a shock tube. It is then easily measured

Although the higher-order effects are likely to be small, it is interesting to see to what extent shock-tube experiments respond to the predictions of the simplest form of steady-state magnetohydrodynamic theory. The later part of the paper describes some measurements of the distortion of a magnetic field.

## 2. Kinematic solution

We shall use the cylindrical polar co-ordinate system  $(r, \theta, z)$  where the  $z$ -axis lies along the axis of the tube. The assumptions discussed in the introduction require that

$$\partial/\partial t = 0, \quad \partial/\partial \theta = 0, \quad \mathbf{B} = (B_r, 0, B_z), \quad \mathbf{v} = (0, 0, v), \quad (4)$$

where the  $z$ -component of the velocity is constant. It is easily seen that the electric field intensity is zero, and the magnetic field can then be found from

$$\operatorname{div} \mathbf{B} = 0, \tag{5}$$

$$\operatorname{curl} \mathbf{B} = \mu \mathbf{j} = \mu \sigma \mathbf{v} \times \mathbf{B}, \tag{6}$$

where we shall assume constant permeability, and  $\mathbf{j}$  is the current density. It is convenient to use the vector potential  $\mathbf{A}$  with the definition

$$\operatorname{curl} \mathbf{A} = \mathbf{B}, \quad \operatorname{div} \mathbf{A} = 0, \tag{7}$$

and to introduce co-ordinates referred to the tube radius  $r_0$

$$R = r/r_0, \quad Z = z/r_0. \tag{8}$$

Then by (4) we have 
$$\mathbf{A} = (0, A, 0), \tag{9}$$

(5) is necessarily satisfied and (6) becomes

$$\frac{\partial^2 A}{\partial Z^2} + \frac{\partial}{\partial R} \left( \frac{1}{R} \frac{\partial (RA)}{\partial R} \right) = 2\lambda \frac{\partial A}{\partial Z}, \tag{10}$$

where  $2\lambda = \mu \sigma v r_0$ . If  $\sigma$  is constant the problem can be characterized by  $\lambda$ , or more naturally by the magnetic Reynolds number based on tube diameter with

$$R_M = 2\mu \sigma v r_0 = 4\lambda. \tag{11}$$

Rearranging (10), we obtain

$$\left( \frac{\partial^2}{\partial Z^2} + \frac{\partial^2}{\partial R^2} + \frac{1}{R} \frac{\partial}{\partial R} + \frac{1}{R^2} - \lambda^2 \right) e^{-\lambda Z} A = 0. \tag{12}$$

For present purposes we seek a solution to (12) of the form

$$A = \int_{-\infty}^{\infty} A_W(Z_W) f(R, Z - Z_W) dZ_W, \tag{13}$$

where  $A_W$  would be the measured value of  $A$  on the tube wall at  $Z = Z_W$ . It should be noted that  $A_W$  is related to the total magnetic flux enclosed by the particular transverse section of the tube. The elementary solution for a small flux element,  $A_W f(Z) \delta Z$ , will have boundary conditions

$$\left. \begin{aligned} A &= A_W \quad \text{at} \quad R = 1, \quad -\frac{1}{2}\delta Z < Z < \frac{1}{2}\delta Z; \\ A &= 0 \quad \text{at} \quad R = 1, \quad Z < -\frac{1}{2}\delta Z, \quad Z > \frac{1}{2}\delta Z. \end{aligned} \right\} \tag{14}$$

The required expression can be found by straightforward Fourier-transform techniques, and the derivation is given in the Appendix. We obtain for the field on the axis of the tube

$$\frac{\delta B_Z r_0}{A_W \delta Z} = \frac{e^{\lambda Z}}{2\pi} \int_{-\infty}^{\infty} \frac{(q^2 + \lambda^2)^{\frac{1}{2}}}{I_1[(q^2 + \lambda^2)^{\frac{1}{2}}]} e^{-iqZ} dq, \tag{15}$$

where  $I_1[(q^2 + \lambda^2)^{\frac{1}{2}}]$  is a modified Bessel function of the first kind and of first order. Although (15) is an exact solution, it is interesting to expand the integrand in powers of  $\lambda$ , and find how many terms would be needed for a reasonable estimate of the field strength using a power series in  $R_M$ .

The expansions for modified Bessel functions of the first kind give

$$\begin{aligned} \frac{I_1[(q^2 + \lambda^2)^{\frac{1}{2}}]}{(q^2 + \lambda^2)^{\frac{1}{2}}} &= \frac{1}{(q^2 + \lambda^2)^{\frac{1}{2}}} \sum_{n=0}^{\infty} \frac{\{\frac{1}{2}(q^2 + \lambda^2)^{\frac{1}{2}}\}^{2n+1}}{n!(n+1)!} = \sum_{n=0}^{\infty} \sum_{m=0}^n \frac{(\frac{1}{2})^{2n+1} q^{2n-2m} \lambda^{2m}}{(n-m)! m! (n+1)!} \\ &= \sum_{m=0}^{\infty} \sum_{n=m}^{\infty} \frac{\lambda^{2m}}{2^m m! q^{m+1}} \frac{(\frac{1}{2}q)^{2(n-m)+m+1}}{(n-m)! \{(n-m) + (m+1)\}!} \\ &= \sum_{m=0}^{\infty} \frac{\lambda^{2m}}{2^m m!} \frac{I_{m+1}(q)}{q^{m+1}}. \end{aligned} \tag{16}$$

We then have

$$\frac{(q^2 + \lambda^2)^{\frac{1}{2}}}{I_1[(q^2 + \lambda^2)^{\frac{1}{2}}]} = \frac{q}{I_1(q)} \left\{ 1 + \sum_{m=1}^{\infty} \frac{I_{m+1}(q)}{q^m I_1(q)} \frac{\lambda^{2m}}{2^m m!} \right\}^{-1} = \frac{q}{I_1(q)} \left\{ 1 - \frac{\lambda^2}{2} \frac{I_2(q)}{q I_1(q)} + O(\lambda^4) \right\}, \tag{17}$$

provided that 
$$\frac{(q^2 + \lambda^2)^{\frac{1}{2}}}{I_1[(q^2 + \lambda^2)^{\frac{1}{2}}]} \frac{I_1(q)}{q} > \frac{1}{2} \quad \text{for all } q. \tag{18}$$

Terms containing  $I_{m+1}(q)/q^m I_1(q)$  in (17) have their maximum values at  $q = 0$ , and hence (18) is satisfied if  $\lambda/I_1(\lambda) > 1$ , which requires  $R_m = 4\lambda < 9.95$ .

Z	0	0.1	0.2	0.3	0.4	0.5
$g_0(Z)$	1.775 (8)	1.723 (0)	1.576 (4)	1.365 (3)	1.126 (3)	0.891 (3)
$g_1(Z)$	0.384 (7)	0.376 (0)	0.351 (4)	0.314 (8)	0.267 (7)	0.226 (0)
	0.6	0.7	0.8	0.9	1.0	1.1
	0.6815	0.5068	0.3688	0.2641	0.1867	0.1307
	0.1831	0.1449	0.1123	0.0858	0.0646	0.0481
	1.2	1.3	1.4	1.6	1.8	2.0
	0.0909	0.0628	0.0433	0.0204	0.0954	0.0045
	0.0356	0.0261	0.0190	0.0100	0.0052	0.0026
	2.2	2.6	3.0			
	0.0021	0.0010	0.0004			
	0.0013	0.0003	0.0001			

The results for which the last figure is given in parentheses may be in error by 0.0002.

TABLE 1

Substituting from (17) in (15), we can obtain

$$\delta B_Z r_0 / A_W \delta Z = e^{\frac{1}{2} R_M Z} \{ g_0(Z) - \frac{1}{3^2} R_M^2 g_1(Z) + O(R_M^4) \}, \tag{19}$$

where  $g_0(Z)$  and  $g_1(Z)$  are even functions of  $Z$  given by

$$g_0(Z) = \frac{1}{\pi} \int_0^{\infty} \frac{q}{I_1(q)} \cos q Z dq, \quad g_1(Z) = \frac{1}{\pi} \int_0^{\infty} \frac{I_2(q)}{I_1^2(q)} \cos q Z dq. \tag{20 a, b}$$

$g_0(Z)$  and  $g_1(Z)$  can also be expressed in series form as can be seen from the alternative expression to (15) derived in the Appendix. However, convergence for small  $Z$  is not rapid. Using the series where possible and the method for numerical integration developed by Filon (1928) where not, the above table (table 1) has been compiled.

Finally, expanding  $e^{R_M Z/4}$  in (19), we obtain the first four terms of the power series solution:

$$\delta B_Z r_0 / A_W \delta Z = g_0(Z) + R_M \frac{1}{4} Z g_0(Z) + R_M^2 \frac{1}{32} \{Z^2 g_0(Z) - g_1(Z)\} + R_M^3 \frac{1}{384} \{Z^3 g_0(Z) - 3Z g_1(Z)\} + O(R_M^4). \quad (21)$$

### 3. Discussion

If the magnetic flux at the wall is held constant for a d.c. coil mounted outside the tube,  $A_W$  is symmetric about the plane of the coil, and decreases monotonically to zero with distance from the coil. Such a variation of  $A_W$  is crudely represented by the boundary conditions (14), and the elementary solution (15) should give an indication of the general features of the magnetic field due to a single d.c. coil. However, when the restriction on magnetic-field changes at the wall is

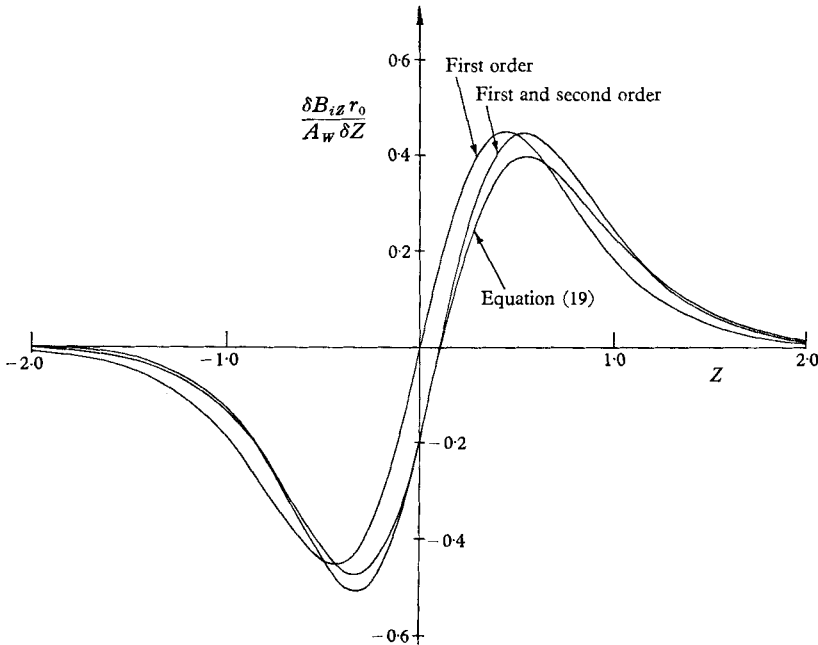


FIGURE 1. Comparison of induced field solutions on the axis of a tube for  $R_M = 4$ .

relaxed, it is likely that field distortion is greater than is indicated here. Figure 1 compares approximate solutions for the induced magnetic field  $\delta B_{iZ}$  on the axis of the tube when  $R_M = 4$ . Values of the applied field  $\delta B_{0Z}$  can be found from the previous table since by (21)  $\delta B_{0Z} r_0 / A_W \delta Z = g_0(Z)$ . Two of the curves in figure 1 are taken from equation (21), and represent solutions correct to first order and second order in  $R_M$ . The remaining curve was calculated from equation (19). A few points were computed from the exact solution and were found to be indistinguishable from the last curve in the figure. The induced field is also quite well represented by the solution correct to third order in  $R_M$ .

The maximum induced field on the axis has a value approximately one-quarter of the maximum applied field. Second- and higher-order effects do not have a great significance when considering the magnetic field as a whole, but they can

be important when measuring the induced field only, as in the experiments on electrical conductivity. However, the second-order term in the solution is zero at  $Z = \pm 0.5$  approximately, points at which the magnitude of the first-order term is nearly maximum. This feature may be guessed intuitively since first-order radial-field components will tend to disappear near where the first-order field on the axis is a maximum; second-order induced currents and axial fields will then be small. When the tube is non-conducting, similar reasoning suggests that second-order flux linkage through an external search coil is zero in the region of maximum first-order flux linkage. The fact that higher-order effects were small in the experiments of Lin *et al.* (1955) might perhaps be due to having the search coil in such a position. In the work of Pain & Smy (1960) two field coils with opposing currents were arranged symmetrically about the plane of the search coil. Second- and all even-order flux linkage would be zero. However, some tests showed a marked variation of conductivity along the length of the gas sample, field strengths were in some cases nearly high enough for dynamic interaction, and the present arguments are hardly justified.

#### 4. Experiments on field distortion

A 5 in. diameter combustion-driven shock-tube was used for experimental measurement of magnetic field distortion. The test-section tube was made of copper, and had a wall thickness of  $\frac{1}{4}$  in. The decay time for a uniform magnetic field in such a tube is approximately 30 msec, as compared to the 0.2 msec maximum duration of ionized gas flow. Tests with an external search coil confirmed that flux changes at the copper were negligible. A weak magnetic field was provided by a short d.c. coil mounted co-axially with the shock tube. The field strength on the axis of the tube was  $5 \times 10^{-3}$  W/m<sup>2</sup>, and the dynamic interaction parameter  $C_M$  based on this field strength and the diameter of the tube was of order  $10^{-2}$ . The applied flux at the wall was measured for a series of transverse sections on a separate test rig.

Two search coils mounted in a non-conducting probe were used to measure the induced field on the axis of the tube. The probe had to be constructed robustly, but the reduction in total flow area due to its presence was only 1%. In order to take a series of induced field readings, the position of the field coil relative to the shock tube could be varied. The search coils were designed to give a large-amplitude signal so that trouble from the electrostatic pick-up noticed by Lin *et al.* (1955) would be avoided. However, a slight pick-up was observed, and had to be allowed for. The signals were integrated before display on an oscilloscope.

Ionization probes detected shock position at four points upstream of the test section, and the time taken for the shock to pass between probes was measured. Uniformity of measured shock velocity was taken as a reasonable indication that flow velocity behind the shock would be uniform. De Leeuw (1958) has tabled values of velocity and electrical conductivity behind strong shocks travelling into argon, which was the working gas in the present case. He assumed that thermal equilibrium is obtained behind the shock, and computed electrical conductivity by the same method as Lin *et al.* (1955). From these results experimental values of  $R_M$  could be estimated.

Test runs were made with shock Mach numbers in the range 11.0–11.3 and in the range 14.2–15.3. Corresponding values of  $R_M$  are 1.5–1.6 and 3.1–3.8. The initial gas pressure was 3 mm of mercury. A third series was attempted for Mach numbers of 17, but conditions were found to be too unsteady. Results are plotted in figure 2, and are compared with theoretical curves for mean values of  $R_M$  in each series. The curves were found by numerical integration, using measured values of  $A_W$  and the solution given by equation (19). It should be

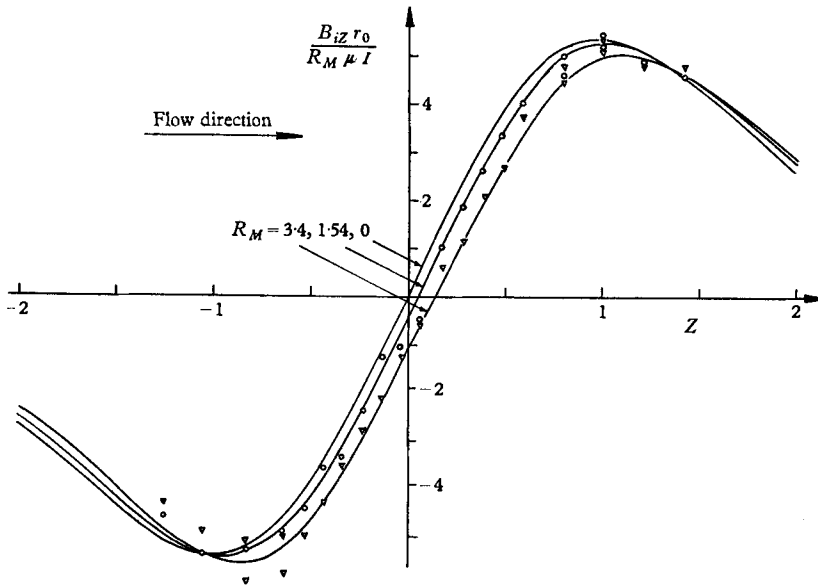


FIGURE 2. Induced field on the axis of the shock-tube. The full lines are calculated from the known flux at the wall. The symbols,  $\circ$  and  $\nabla$ , designate experimental readings taken for  $R_M$  in the region of 1.54 and 3.4, respectively.  $I$  refers to current in the d.c. coil.

noted that, in order to close the scale of the graph, the induced field has been divided by  $R_M$ . All experimental points have been scaled by a further factor of 0.94. The absolute calibration of the search coils was only of this order of accuracy although their relative calibration was better. The arbitrary reduction of the experimental values has been done to emphasize the fact that in relation to each other the results of each series show the expected trend. Scatter of the points is due to experimental errors rather than variations of  $R_M$  within the test ranges.

A typical oscilloscope trace is shown in figure 3. Although relaxation times for ionization were greater in the low Mach number series, equilibrium appeared to be reached in all runs. The purity of the argon was approximately 99%, a fact which may account for the rapid ionization. It is not expected that the presence of impurities would seriously affect the estimates of conductivity. Between the initial rise of induced field and the cut-off with the advent of the driver gases at the contact 'front', the oscilloscope trace shows a gradual decay on which a slight ripple is superimposed. The decay is due to radiation cooling lowering the gas conductivity. The ripple is slightly greater than that expected from typical variation in measured shock velocity. Lin *et al.* (1955) observed a

similar effect, and have suggested that it is due to radial oscillatory motion of the gas interacting with longitudinal field components. In measuring the magnitude of the signal an estimate was made of the shape of the trace if the ripple were discounted, and the reading was taken at a point before decay had become appreciable.

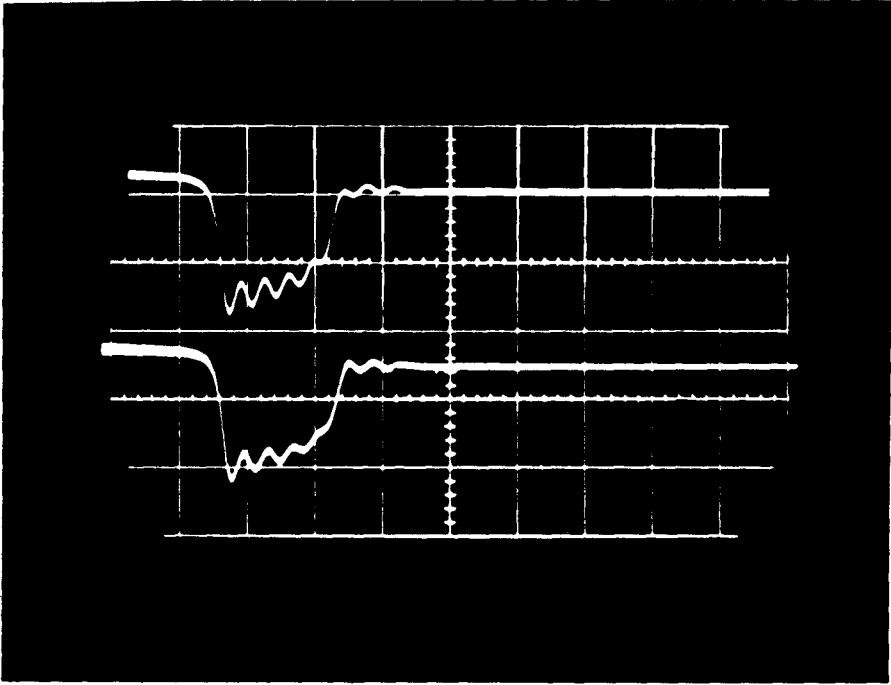


FIGURE 3. Typical oscilloscope trace of integrated signals from the search coils. Shock Mach number 15.2, time scale  $40 \mu\text{sec/cm}$ . For the upper trace the search coil was at  $Z = -0.84$ , and for the lower at  $Z = -0.64$ .

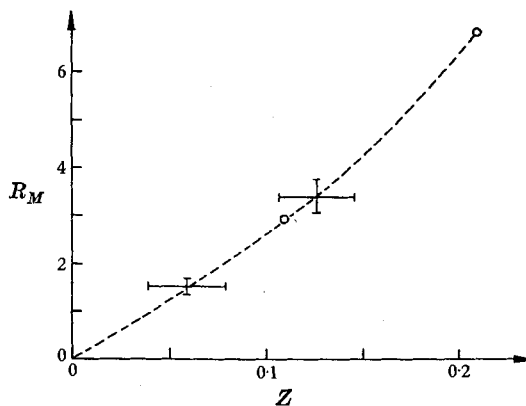


FIGURE 4. Displacement of the point on the axis of the shock-tube at which the induced field is zero. Points calculated from the solution correct to third order in  $R_M$  are shown by the symbol  $\circ$ . Points taken from the experimental curves are shown with the expected range of error by the elongated crosses.



The position at which the induced field is zero is moved progressively downstream as  $R_M$  increases. The determination of this point experimentally for each series is not affected by systematic errors in the reading of the magnitude of induced fields. This displacement was estimated from curves giving the best fit to the experimental points. The results are compared in figure 4 with points calculated for the solution correct to third order in  $R_M$ .

The author is greatly indebted to Dr J. A. Shercliff for many stimulating discussions during the course of the work and to Mrs P. Camm for her help in computing results. The shock-tube project is supported by the United Kingdom Atomic Energy Authority.

**Appendix: Derivation of the magnetic field solution**

Let  $\mathcal{A} = e^{-\lambda Z} A$ , and  $\bar{\mathcal{A}}(q)$  be the Fourier transforms of  $\mathcal{A}$ , so that

$$\bar{\mathcal{A}}(q) = \int_{-\infty}^{\infty} \mathcal{A} e^{iqZ} dZ.$$

If we assume  $\mathcal{A}$  and  $\partial\mathcal{A}/\partial Z \rightarrow 0$  as  $|Z| \rightarrow \infty$ , and defer justification until later, (12) becomes

$$\left\{ \frac{\partial^2}{\partial R^2} + \frac{1}{R} \frac{\partial}{\partial R} + \frac{1}{R^2} - (q^2 + \lambda^2) \right\} \bar{\mathcal{A}} = 0. \tag{22}$$

The appropriate solution for the field inside a tube is

$$\bar{\mathcal{A}} = C I_1[(q^2 + \lambda^2)^{\frac{1}{2}} R], \tag{23}$$

where  $C$  is a constant. The transform of the boundary conditions (14) gives, at  $R = 1$ ,

$$\delta \bar{\mathcal{A}} = \int_{-\frac{1}{2}\delta Z}^{\frac{1}{2}\delta Z} e^{-\lambda Z} A_W e^{iqZ} dZ \rightarrow A_W \delta Z, \text{ as } \delta Z \rightarrow 0. \tag{24}$$

Using (24) in (23) to evaluate  $C$ , and inverting, we obtain

$$\frac{\delta A}{A_W \delta Z} = \frac{e^{\lambda Z}}{2\pi} \int_{-\infty}^{\infty} \frac{I_1[(q^2 + \lambda^2)^{\frac{1}{2}} R]}{I_1[(q^2 + \lambda^2)^{\frac{1}{2}}]} e^{-iqZ} dq. \tag{25}$$

The magnetic field on the axis of the tube is then given by

$$\frac{\delta B_Z r_0}{A_W \delta Z} = \frac{e^{-\lambda Z}}{2\pi} \int_{-\infty}^{\infty} \frac{(q^2 + \lambda^2)^{\frac{1}{2}}}{I_1[(q^2 + \lambda^2)^{\frac{1}{2}}]} e^{-iqZ} dq. \tag{26}$$

The path of integration for (26) can be closed in the complex  $q$ -plane by a curve where  $iq \rightarrow \infty$  if  $Z > 0$ , or where  $iq \rightarrow -\infty$  if  $Z < 0$ . The poles of the integrand lie at  $q = \pm i(\lambda^2 + \alpha_s^2)^{\frac{1}{2}}$  where  $\alpha_s$  is any of the roots of  $J_1(\alpha) = 0$ , except for  $\alpha = 0$ , and  $J_1(\alpha)$  is a Bessel function of the first kind and of the first order. The sum of the residues at the poles in the appropriate half plane gives

$$\frac{\delta B_Z r_0}{A_W \delta Z} = -e^{\lambda Z} \sum_{s=1}^{\infty} \frac{\alpha_s e^{-(\lambda^2 + \alpha_s^2)^{\frac{1}{2}} |Z|}}{(\lambda^2/\alpha_s^2 + 1)^{\frac{1}{2}} J_0(\alpha_s)}. \tag{27}$$

A similar series can be formed for the integral in (25), and it is found that the original assumptions,  $\mathcal{A}$  and  $\partial\mathcal{A}/\partial Z \rightarrow 0$  as  $|Z| \rightarrow \infty$ , are justified. The integral of (26) is expanded as a power series in §2. The series for the individual terms are most easily obtained by expanding (27).

## REFERENCES

- COWLEY, M. D. 1961 *Quart. J. Mech. Appl. Math.* **14**, 319.  
DE LEEUW, J. H. 1958 *U.T.I.A. Rep.* no. 49, Toronto University.  
FILON, L. N. G. 1938 *Proc. Roy. Soc. Edinb.* **49**, 38.  
LIN, S. C., RESLER, E. L. & KANTROWITZ, A. 1955 *J. Appl. Phys.* **26**, 95.  
LUNDQUIST, S. 1952 *Ark. Fys.* **5**, 297.  
PAIN, H. J. & SMY, P. R. 1960 *J. Fluid Mech.* **9**, 390.